Techno-Economic Analysis of Battery Electricity Storage Towards Self-Sufficient Buildings.

Alessandro Rosati[1], Andrea L. Facci[a,*], Stefano Ubertini[1]

[a]*Department of Economics, Engineering, Society and Business Organization, University of Tuscia, 01100 Viterbo, Italy.*

Abstract

Effective electricity storage solutions that decouple energy use and production are central to the green energy transition. In particular, in the residential sector, the implementation of such solutions should boost the potential of nearly zero energy buildings to reduce the primary energy consumption and greenhouse gases emission and towards a greater energy self-sufficiency.

The aim of this paper is to assess a climate independent scaling law for the introduction of a battery energy storage in a residential environment. To this end, we evaluate the environmental and economic impact of the integration of a lithium-ion battery in a real existing residential building, for different climates and for different battery capacities. The building is made of 13 apartments and features a reversible heat pump, a photovoltaic system, and a lithium-ion battery. We model all the elements and the energy consumption of the building and validate results against measured data.

The results show that sizing the lithium-ion battery based on the variation of the self-consumed renewable energy yields a sustainable investment for all climates. Moreover, from a techno-economic perspective, lithium-ion batteries are better suited for daily energy storage rather than seasonal storage. In fact, they efficiently fill the time lag between demand and production on a daily time scale. On the other hand, lithium-ion battery costs gathers unsustainable investments for seasonal storage also considering any foreseeable battery cost reduction. Optimized building-level battery storage cannot fill completely the temporal mismatch between production and usage. As a consequence, different technologies (e.g. electric mobility) should be also considered to locally consume all the energy produced by the photovoltaic.

Keywords: Electrical Storage, Lithium-Ion battery, Nearly Zero Energy Buildings, Techno-Economic Analysis, Renewable Energy.

1. Introduction

The growing concerns about climate change, fossil fuel shortage, and air pollution are driving the energy transition towards a sustainable energy sector based on Renewable Energy Sources (RES) [1]. The European Commission has set to reduce GreenHouse Gas (GHG) emissions to at least 40% below the 1990 level by 2030 [2]. Furthermore, in December 2015, the 21^{st} session of the Conference of the Parties to the United Nations Framework Convention on Climate Change in Paris ended with the landmark agreement to reduce GHG emissions by 80% by 2050, to enhance the use of RES, and to improve energy efficiency [3].

In this context electricity generation is becoming more distributed and multi-energy systems are increasingly popular. They leverage on the interaction between different energy carriers (e.g. electricity, hydrogen, and heat) to enhance the economic, technical, and environmental performance [4–6]. Their operation is strongly based on the use of RES, whose availability is often time and weather dependent (e.g. solar and wind power). This intermittent nature causes several issues to the operation and the stability of the power system [7–10] and requires to increase the flexibility of the whole energy system [11–13]. This can be achieved by switching to "intelligent" networks (smart grids) capable of managing and regulating multiple electrical streams that flow in a discontinuous and bidirectional manner [14–18], through demand side management, and through the implementation of energy storage systems [11, 19].

The concepts of energy and time are tightly connected. In this respect, shifting demand to match supply and reconceptualizing interactions between time and energy is pivotal to achieve low-carbon energy goals [20–22]. As a consequence, the design of new energy systems must rely on real time-varying consumption data, rather than on peak or average demands to allow the contemporary optimization of production and demand phases [23–27]. In this scenario, load control technologies (i.e. storage technologies) able to reshape customer load profiles with the aim to optimize the use of RES [28] are central. Such storage technologies still need a co-evolution of innovation, investment, and deployment strategies [29]. This, highlights a significant knowledge gap on techno-economic assessment of electricity storage systems. Such analyses should draw general scaling laws for the optimized design of electricity storage systems that aim at optimally allocating the energy and financial resources.

*Corresponding author. Tel.: +39 0761 357676.

Email addresses: alessandro.rosati@unitus.it (Alessandro Rosati), andrea.facci@unitus.it (Andrea L. Facci), stefano.ubertini@unitus.it (Stefano Ubertini)

Among the different energy storage solutions, Battery Energy Storage Systems (BESSs) are the most widespread technology [30–32]. Batteries are used in a wide range of applications such as energy storage, electric utility, portable devices, and electric vehicles [30–34]. They have drawn considerable attention thanks to favourable features, such as fast response, controllability, and geographical independent operation [35, 36]. The integration of RES and BESSs is an effective approach to solve the temporal mismatch between production and use, and to perform peak shaving, load leveling, demand response, voltage regulation, frequency regulation, and other ancillary services [37–41]. Batteries can also reduce the cost of electricity in commercial buildings and residential dwellings by absorbing and storing energy from the grid during off-peak periods and injecting it during high-demand periods when prices are very high [42, 43]. However, their investment cost is still high [44] even though in the last decade the price of Lithium-Ion (Li-Ion) batteries has fallen, and this trend is expected to continue [45].

In 2012 the contribution of buildings to the final energy consumption in Europe was 40%, making the building stock responsible for 36% of the total European CO_2 emissions [46]. Over the years, the buildings share of the final energy consumption has remained fairly stable and in 2017 it stood at around 42% [47]. Since 2007, stringent building codes and policies caused this value to decrease slightly in residential buildings. Conversely, the final energy consumption in non-residential buildings remained stable over the last decade [46]. In commercial buildings, high consumption ordinarily occurs during the daytime, when the PhotoVoltaic (PV) production also peaks. Instead, in residential buildings the consumption is usually lagged in time with respect to PV production. As a consequence they are excellent candidates for increasing self-consumption thanks to the use of BESSs [48, 49]. Such considerations highlight that it is necessary to refurbish existing buildings and to design new ones with low energy demand, availability of RES, and electricity storage [50–53]. In the last decade new policies have introduced technical and regulatory measures to promote a more rational energy use in the residential compartment [54–56]. One key is the introduction of nearly Zero Energy Buildings (nZEB) concept as the new building target [57–61]. A nZEB is a building with a very high energy performance, where the nearly zero or the very low amount of energy required is covered to a very significant extent by energy from renewable sources produced on-site or nearby [62].

In such a building environment, Li-Ion battery systems are particularly suited to achieve high self-sufficiency, see for instance [63]. Therein, three different types of batteries, including lead acid, NaNiCl (Sodium-Nickel-Chloride) and Li-Ion, are studied in combination with PV within the Swedish context. Similarly, several studies focus on techno-economic analysis of BESS in residential buildings in specific energy markets and climates. In particular, in the Australian energy market combining PV and BESS gathers a sustainable investment [64]. In Finland, BESS is demonstrated to increase the PV optimal size for both apartment and detached houses [11]. However, such a result is subject to the adoption of dedicated energy pricing policies. In the same way, for the United States energy market sustainability of the investment of BESS combined with PV still relies on the implementation of financial support mechanisms [65]. The profitability of combining PV and BESS in the residential environment depends on the possibility to significantly increment renewable energy self consumption [66]. This also evidence the importance of selecting a proper control strategy [67, 68]. The relevance of such a control strategy is demonstrated for a multi energy system in Hong Kong [67] and for a low energy building in China [68].

Despite site-specific studies clearly evidence the usefulness and profitability of the BESS in the residential setting, to the best of our knowledge, climate independent general scaling laws are still not established. In this paper we posit the challenge to determine such scaling laws by dissecting the behaviour of a whole nZEB for different climatic conditions and BESS capacities. We model all the elements of the system (residential building, reversible heat pump, PV, and Li-Ion battery). Specifically, we consider the BESS performance as a function of the State of Charge (SoC) and temperature, and its thermal management and geometry. High resolution measured energy demands are only sparsely available due to the limited diffusion of smart energy meters in residential settings and privacy concerns [69, 70]. Thus, we determine the nZEB energy demand through a thermodynamic building model validated by comparison against site-specific measures.

The paper is organized as follows. The problem statement is presented in Section 2. In Section 3 we describe the system, its control logic, and the numerical models. Results are presented and discussed in Section 4. Finally, in Section 5, we draw the conclusions.

2. Problem Statement

In this paper we dissect the environmental and economic impact of the integration of a Li-Ion battery-based electricity storage in a residential setting (Fig. 1), for different climates and with different battery capacities. We analyze a year of system operation for the five different climates with a hourly time discretization.

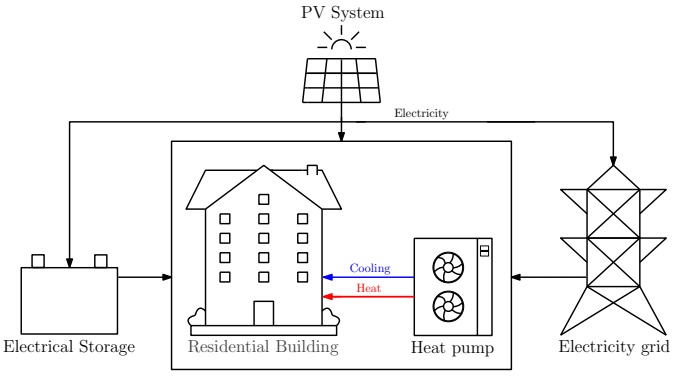

Figure 1: Schematic representation of the main elements of the system.

We consider a building designed following the "Directive of the European Parliament on the energy performance of building" $(2010/31/EU)$ [71] and that meets the "Casaclima" en-

ergy certificate [72]. It belongs to the CasaClima A energy class (Class A for what concerns the envelope efficiency, Gold Class for what concerns the overall energy efficiency). It can be considered as a nZEB, and it is representative of future energy communities, in particular in a context of distributed generation [73]. The building is located in Viterbo, Italy, and is equipped with energy meters that allow to validate its modeling. Its main features are shown in Table 1. The building integrated PV (Fig. 1) utilizes 75% of the total building roof, for a peak power $P_{peak} = 38.6\,\text{kWp}$. A $42\,\text{kW}$ centralized reversible heat pump system provides cooling and heating energy (Fig. 1). Notably, such a system converts heat and cooling loads into an electricity demand, and the nZEB requires no fuels.

Feature	Value	Unit of Measure
Surface	1314	m^2
Floors	6	–
Apartments	13	–
Roof Surface	263	m^2

Table 1: Relevant properties of the selected building reported in the "Casaclima" energy certificate.

Electricity is stored in Li-Ion pouch cell batteries (i.e. those used in the Nissan Leaf car) whose main characteristics, according to the $IEC\,62660-1$ [74], are shown below in Table 2. Battery capacity is varied by changing the arrangement and number of cells.

Feature	Value	Unit of Measure
Rated capacity	56.3	Ah
Nominal voltage	3.65	V
Lenght	261	mm
Width	216	mm
Thickness	7.91	mm
Mass	914	g
Energy density	224	Wh/kg

Table 2: Relevant properties of the Li-Ion pouch cells, according to $IEC\,62660-1$ [74].

Environment temperature influences heating and cooling energy demands and, consequently, the interaction between the PV, the battery, and the electricity grid. To dissect such an influence, we consider five different climates, according to the International Energy Agency (IEA) classification [75]: Cold, Heating based, Moderate, Cooling based, and Hot. The IEA classifies the climatic conditions according to the total number of Heating Degrees Days (HDD) and Cooling Degrees Days (CDD) per year, as reported in Table 3. Therein, we also report a representative European city for each climate.

3. Modelling and Description of the system

3.1. Energy fluxes

The system bidirectionally interacts with the electricity grid as evidenced in Fig. 1 and 2. The load is first satisfied by the PV system. When its production is larger than demand, the surplus energy is sent to the battery and, once its maximum SoC is reached, to the grid. If the building consumption is greater than the PV production, the necessary energy is first drawn from the battery. When it is discharged, the grid feeds the required power.

Climatic Zone	HDD [°C]	CDD [°C]	City
Cold	≥ 2000	≤ 500	Warsaw (Poland)
Heating based	≥ 2000	$[500, 1000]$	Viterbo (Italy)
Moderate	≤ 2000	≤ 1000	Malaga (Spain)
Cooling based	$[1000, 2000]$	≥ 1000	Athens (Greece)
Hot	≤ 1000	≥ 1000	Larnaca (Cyprus)

Table 3: Heating and Cooling Degrees Days and representative cities for each IEA climatic zone [75].

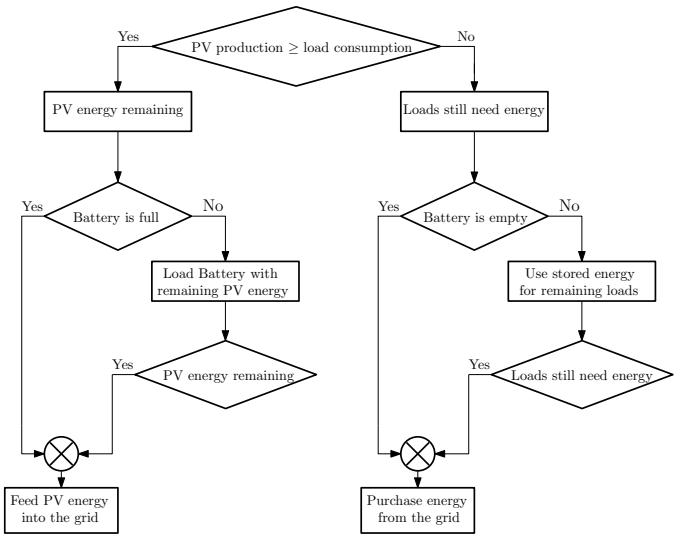

Figure 2: Representation of the nZEB energy fluxes control logic.

3.2. Residential Building

We model the building through the "EnergyPlus" software [76]. It uses a thermodynamic approach based on energy and mass balance equations [76]. The building can be divided into different zones based on their usage and required temperature. The model inputs are: (i) the geometry of each building zone; (ii) the envelope properties; (iii) the activities (e.g appliances and lighting schedule) related to each zone; (iv) the temperatures that must be guaranteed in each zone; (v) the characteristics of the heat pump. Finally, a Typical Meteorological Year (TMY) provides all the meteorological data for each location. The outputs are the hourly electricity and HVAC energy demands for each building zone for a calendar year.

Apartments require electricity for lighting, appliances, and HVAC. Fig. 3 shows the lighting and appliances consumption of an apartment (u_{el}) calculated through EnergyPlus for one week. On weekdays, it shows a repetitive daily trend with a peak in the morning and one in the evening. Weekends show three peaks per day: one in the morning, one at lunchtime,

and one in the evening. The morning peak occurs earlier on weekdays than on weekend, as tenants get up earlier to go to work. On weekends, tenants spend more time at home and consume more energy, as arguable from the lunchtime peak and the longer duration of the evening peak compared to weekdays. The u_{el} time trace consistently repeats for all weeks of the year being excessively repetitive compared to real energy demands. Moreover, all the apartments have the same u_{el}.

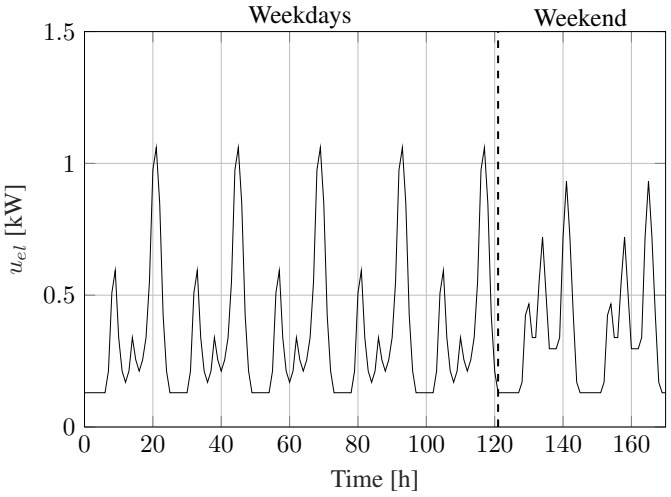

Figure 3: Weekly appliances ad lighting consumption (u_{el}) of an apartment in the building.

To gather a more realistic demand we refer to the electricity demand of the i^{th} apartment:

$$u^*_{el,i}(t) = u_{el}(t) + \sigma_i(t)\,, \tag{1}$$

where $\sigma_i(t)$ is a Gaussian white noise and t is time. Such a procedure does not impact the total energy consumption as σ has zero average. We estimate the amplitude of σ_i from the electricity consumption data reported in [69]. Specifically, we decompose each consumption profile (u) as:

$$u(t) = \bar{u}(t) + u'(t)\,, \tag{2}$$

being $\bar{u}(t)$ the phase average:

$$\bar{u}(t) = \frac{1}{7}\sum_{0}^{6}\left(u(t) + u(t+24)\right)\,. \tag{3}$$

Fig. 4 reports the consumption deviation from phase average ($u'(t)$) relative to the data in Fig. 1 and 9 of [69]. We assume that the amplitude of σ_i equals $\max(u'(t)) = 0.6\,\text{kW}$. The resulting $u^*_{el,i}(t)$ is exemplified in Fig. 5.

We add the HVAC consumption to obtain the total electricity demand of each apartment ($u_{tot,i}$) :

$$u_{tot,i}(t) = u^*_{el,i}(t) + \frac{u_{h,i}(t)}{\text{COP}_h} + \frac{u_{c,i}(t)}{\text{COP}_c}\,, \tag{4}$$

where $u_{h,i}$ and $u_{c,i}$ are the heat and cooling demands respectively, while COP_h and COP_c are the heat pump Coefficients Of Performance for heating and cooling operations, respectively.

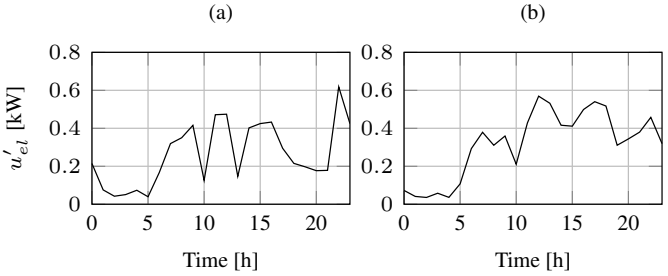

Figure 4: Consumption deviation from phase average relative to (a) the data in Figures 1 of [69]; (b) the data in Figures 9 of [69].

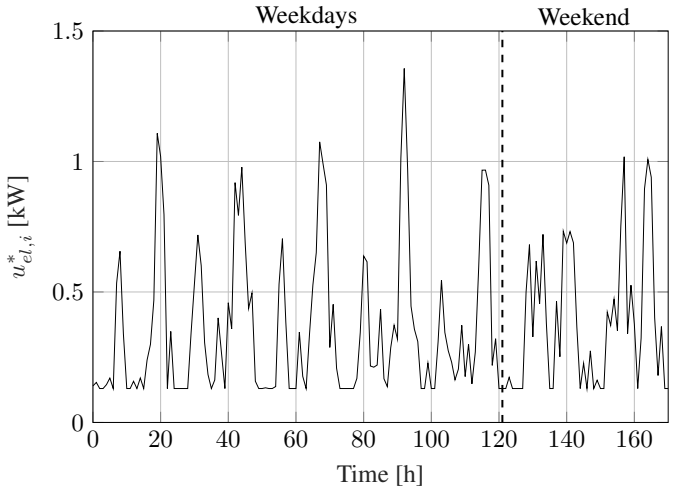

Figure 5: Modified weekly appliances ad lighting consumption ($u^*_{el,i}$) of an apartment in the building.

Finally, the total electricity demand (u_{tot}) is the sum of all the $u_{tot,i}$ and of the lighting consumption of the common areas of the building.

The obtained energy demand is validated for the heating based climate. Table 4 compares the model results to measured data and to the "Casaclima" energy certificate requirements for the yearly consumption of electricity for appliances and lighting (U_{el}) , heating (U_h) , and cooling (U_c) .

	Building Model	Measured Data	"Casaclima" Data
U_{el} [kWh]	42856	46319 [77]	38000
U_h [kWh]	7099	6013.3	6574
U_c [kWh]	15426	15898	//

Table 4: Consumption data obtained, measured, and reported in the "Casaclima" energy certificate for the residential building in the Heating based climate.

Measured data for U_{el} are not available for the present building. Yet, the obtained value is consistent because it is included between the consumption reported in the "Casaclima" energy certificate and the one reported in [77] for a similar residential building (with the same number of apartments). U_h is slightly higher than the measured data and that of the "Casaclima" certificate. U_c is the same as that measured in the residential build-

ing. The "Casaclima" certificate, does not report data for U_c.

PV production (P_{pv}) , is estimated through the "PVGIS" platform for each considered locations [78].

3.3. Battery

The battery is made of Li-Ion pouch cells, whose characteristics are shown in Table 2. We model the cell through the zero-th order equivalent circuit presented in [79] (Fig. 6).

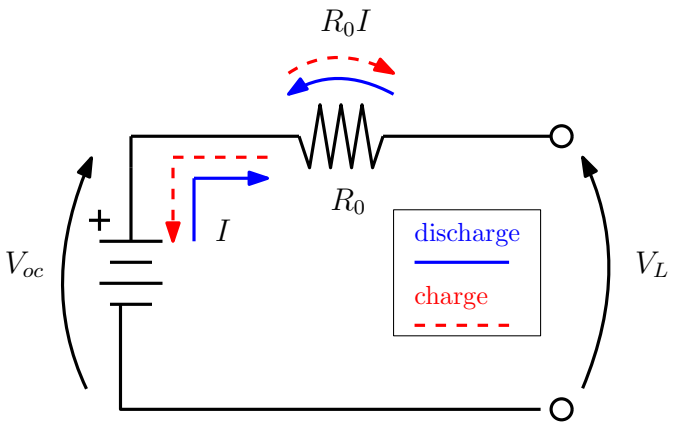

Figure 6: Zero-th order electrical circuit model of the battery [79].

This model demonstrated to be adequate for estimating the losses that occur during battery operation [80, 81]. We assume that at time t the current flowing in and out of the battery terminals (I) , the battery temperature (T) and the SoC are known. For the battery charging process I is negative. Conversely, for the discharge process it is positive. The battery load voltage (V_L) is defined as:

$$V_L(t) = n_s[V_{oc}(t) - R_0(t)I(t)n_p]\,, \tag{5}$$

where n_s is the number of cells arranged in series, n_p is the number of cells arranged in parallel, V_{oc} is the open-circuit voltage, and R_0 is the equivalent resistance of the battery. R_0 varies as a function of the temperature and of the SoC (Fig. 7). The effects of temperature on all the other parameters are neglected. For V_{oc}, this assumption is supported by experimental results [82], as evidenced in Fig. 8. The internal resistance of the cell ($\mathcal{R}_i$) is

$$\mathcal{R}_i(t) = \Omega_{\text{cell}} R_0(t)\,, \tag{6}$$

being Ω_{cell} its volume. The heat generated per unit volume (q_{gen}) is determined through eq. 7.

$$q_{gen}(t) = \mathcal{R}_i(t)\frac{I(t)^2}{\Omega_{cell}^2} - \frac{I(t)}{\Omega_{cell}} T(t)\frac{\Delta S(t)}{\mathcal{F}}\,, \tag{7}$$

where $\mathcal{F} = 96485\,\text{C/mol}$ is the Faraday constant and ΔS is the entropy variation that is calculated as a function of the SoC through the experimental formulations presented in [83] and reported in eq. 8.

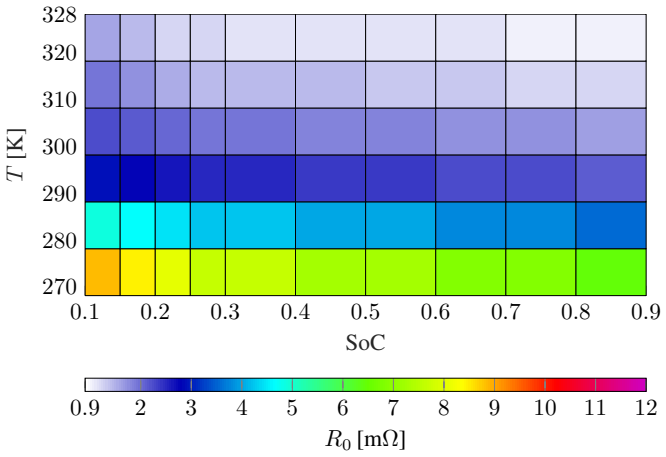

Figure 7: Equivalent resistance of the battery as a function of the temperature and of the SoC.

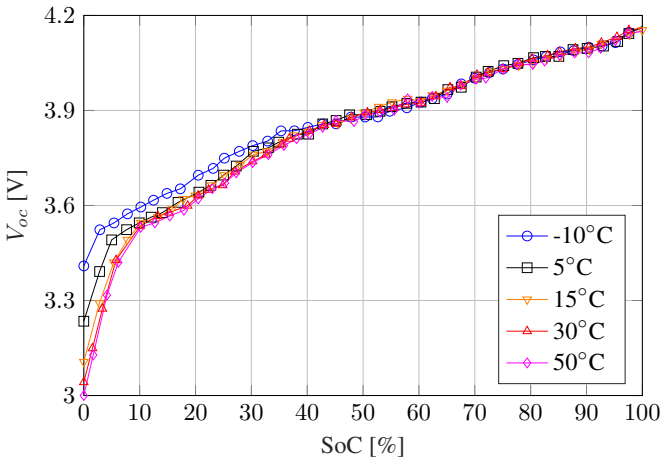

Figure 8: Experimentally validated open-circuit voltage curves as a function of the SoC for different temperatures [79].

$$\Delta S(t) = \begin{cases} 99.88\,\text{SoC}(t) - 76,67 & \text{if} \\ & 0 \le \text{SoC}(t) \le 0.77 \\ -30 & \text{if} \\ & 0.77 < \text{SoC}(t) \le 0.87 \\ -20 & \text{if} \\ & 0.87 < \text{SoC}(t) \le 1 \end{cases} \tag{8}$$

The current $I(t+dt)$ is obtained as

$$I(t+dt) = \pm\frac{V_L(t) - \sqrt{V_L(t)^2 - 4P_{batt}(t)R_0(t)}}{2R_0(t)}\,, \tag{9}$$

where P_{batt} is the electrical power flowing in or out of the battery. The temperature of the battery $T(t+dt)$ is

$$T(t+dt) = T(t)\frac{q_{gen}(t) - \frac{q_{conv}(t)}{\Omega_{batt}}}{c_{p_{cell}}\,\rho_{cell}}, \tag{10}$$

where $c_{p_{cell}}$ is the specific heat capacity, ρ_{cell} is the density of the Li-Ion cell, Ω_{batt} is the volume occupied by the cells within

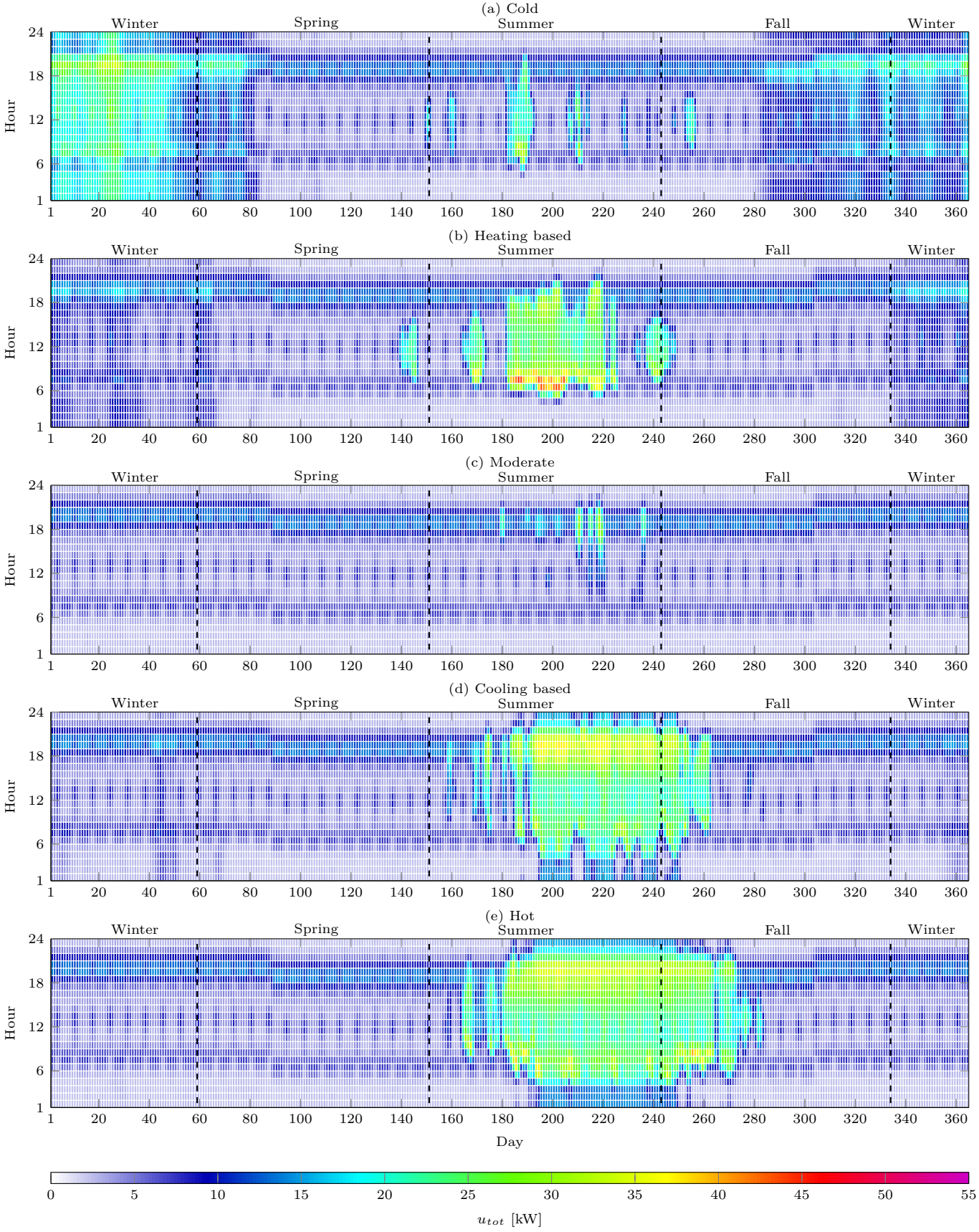

Figure 9: Total building energy consumption as a function of time for (a) Cold climate; (b) Heating based climate; (c) Moderate climate; (d) Cooling based climate; (e) Hot climate.Numerical data can be found at 10.5281/zenodo.5816951.

the battery pack, and q_{conv} is the heat exchanged by natural convection at the battery surface (A) . Specifically,

$$q_{conv}(t) = hA[T(t) - T_{\infty}]\,, \tag{11}$$

being h the convective coefficient and T_{∞} is the environment temperature. Leveraging on the geometry of the Nissan Leaf battery pack [84], we calculate A assuming an effective pack volume equal to $4\,\Omega_{batt}$. We estimate the $\mathrm{SoC}(t+dt)$ through the following eq. 12

$$\mathrm{SoC}(t+dt) = -\frac{I(t+dt)}{Q_{nom}}\eta_c + \mathrm{SoC}(t)\,, \tag{12}$$

where η_c is the Coulomb's efficiency [85] and Q_{nom} is the battery nominal capacity that varies as a function of the number of cells and their arrangement. To ensure correct operation and long battery life, and according to [86], companies like Hitachi, Saft and Solom recommend limiting the SoC variation to the range $0.1 < \mathrm{SoC} < 0.9$.

The model is implemented in the Matlab Simulink computational environment. Each simulation requires few seconds on a state-of-the-art desktop computer (intel-i7 8^{th} generation, 16 Gb RAM).

4. Results and discussion

4.1. Results

Table 5 reports the relevant consumption properties for each climate. In literature, the total annual energy consumption per unit area ($\mathbf{u}_a$) is often retrieved through building simulation models implemented in EnergyPlus, and ranges from a minimum of $30.24\,\mathrm{kWh/m^2}$ [87] to a maximum of $88.67\,\mathrm{kWh/m^2}$ [88]. We comment that, our results, are consistent with this range for all the considered climates.

Climatic Zone	U_{el} [kWh]	U_h [kWh]	U_c [kWh]	$\mathbf{u}_a$ [kWh/m^2]
Cold	42856	38028	3886	64.51
Heating Based	42856	7099	15426	49.76
Moderate	42856	813	1567	34.42
Cooling Based	42856	2132	28486	55.92
Hot	42856	820	37779	61.99

Table 5: Building energy consumption for each climate.

Fig. 9 shows u_{tot} as a function of time for the five considered climates. We observe that in the cold climate the highest consumption is in winter whereas in the hot climate it is in the summer and at the beginning of the fall period. The heating based and cooling based climates exhibit similar trends and air conditioning during the summer is a relevant energy expenditure in both cases. In the heating based climate, consumption in the winter period is, as expected, higher than in the cooling based climate. Finally, for the moderate climate demand is constant throughout the year without significantly dominant periods unlike the other four.

Table 6 reports the relevant model results for the photovoltaic system. Therein, the renewable energy penetration factor is defined as $F = E_{pv}/U_{tot}$, where $U_{tot} = U_{el} + U_h + U_c$. We comment that $F < 1$ for all climates, except for the moderate one. For this particular type of climate, E_{pv} exceeds U_{tot}.

Climatic Zone	E_{pv} [kWh]	F	P_{max} [kW]
Cold	40699	0.48	32.91
Heating Based	57434	0.88	32.72
Moderate	65856	1.46	34.75
Cooling Based	62404	0.85	34.30
Hot	64832	0.80	33.25

Table 6: Relevant properties of the PV system as a fucntion of climate.

For each climate we study the annual behavior of the system for $n = 12$ different battery capacities: $Q_{nom,i} = [0\,\mathrm{kWh}$ (no battery), $40\,\mathrm{kWh}$, $50\,\mathrm{kWh}$, $60\,\mathrm{kWh}$, $70\,\mathrm{kWh}$, $80\,\mathrm{kWh}$, $100\,\mathrm{kWh}$, $120\,\mathrm{kWh}$, $140\,\mathrm{kWh}$, $160\,\mathrm{kWh}$, $215\,\mathrm{kWh}$, $270\,\mathrm{kWh}]$. Specifically, we seek to assess the optimal capacity of the BESS to promote the local self-consumption of the PV energy by filling the time lag between demand and production. To this aim, Fig. 10(a) represents the self-consumed energy (E_s) , that is the energy produced by the photovoltaic system effectively used to satisfy the consumption of the residential building, as a function of the relative battery capacity Θ , defined as

$$\Theta = \frac{Q_{nom}}{P_{max}}\,, \tag{13}$$

being P_{max} the maximum power of the PV. Note that P_{max} differs from the P_{peak} (Table 6).

E_s is a significant parameter both from an energy and system point of view. In fact, it should be maximized to enhance the value of locally produced energy, to minimize grid issues related to renewable energy sources fluctuations, and to minimize energy losses. As expected, the cold climate has the lowest E_s, having the lower E_{pv}. Conversely, the hot climate being characterized by a high E_{pv} and a high U_{tot} has the highest E_s. The moderate climate has the highest E_{pv} but also the lowest U_{tot}. Therefore its E_s is relatively low.

Despite in Fig. 10(a) all the curves relative to different climates qualitatively exhibit the same trend, the different $\max(E_s)$ associated to each climate hinders a general analysis of the battery electricity storage impact.

The same results are reported in Fig. 10(b) through a different parameter space that gathers more insights into the BESS optimal sizing. Specifically, we define the relative variation of self-consumed energy (λ) as:

$$\lambda_i = 100 \times \frac{E_s(Q_{nom,i}) - E_s(Q_{nom,i-1})}{E_{pv}}\,. \tag{14}$$

Notably, in Fig. 10(b), the patterns relative to all climates collapse on the same trend allowing a general analysis of the battery storage optimal sizing and operation. For all the climates, λ is a decreasing function of Θ. On average, $\lambda \simeq 20\%$ for $\Theta = 1.2\,\mathrm{h}$. Such a figure suddenly drops to $\lambda \simeq 5\%$ for $1.5\,\mathrm{h}$

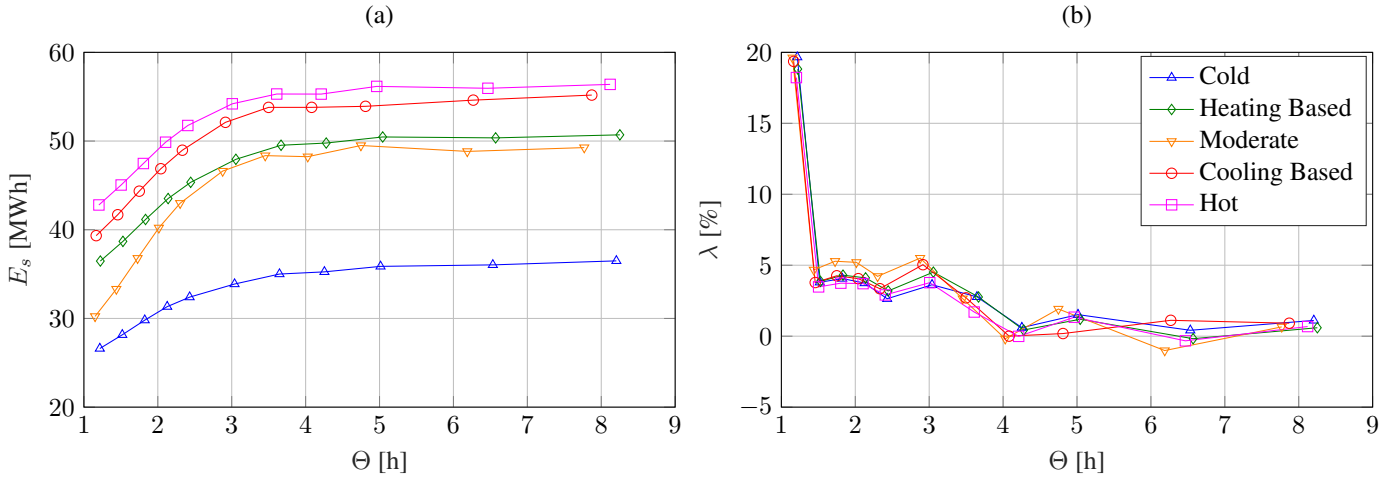

Figure 10: (a) Self-consumed energy as a function of Θ; (b) λ as a function of Θ.

$< \Theta < 3\,\mathrm{h}$. After a relatively flat pattern for $1.5\,\mathrm{h} < \Theta < 3\,\mathrm{h}$, λ reduces to negligible values for $\Theta > 4\,\mathrm{h}$. In summary, $\Theta > 4\,\mathrm{h}$ is not recommended in terms of capacity of the battery storage to increase the renewable energy self consumption while $\Theta = 3.5\,\mathrm{h}$ can be safely considered an energy-system optimal solution. As a consequence, BESS is suitable to fill the daily temporal discrepancy between production and demand. Conversely, seasonal electricity storage would require much larger Θ not gathering significant benefits in terms of self-consumed renewable energy. Fig. 10(a) shows that E_s reaches a plateau as Θ increases. For all climates, such a plateau is below E_{pv} evidencing that a portion of the locally produced renewable electricity is always fed to the grid (even for large Θ). Such an energy varies between $4200\,\mathrm{kWh}$ (cold climate) and $16500\,\mathrm{kWh}$ (moderate climate) and could be stored for later use by exploiting other storage systems.

In 2020, the average cost of the electricity withdrawn from the grid in Europe, was $c_e = 0.2134\,€/\mathrm{kWh}$, including all taxes and levies [89]. Being C_w the total yearly cost of energy withdrawn from the grid, we define γ as:

$$\gamma = 100 \times \frac{C_w(Q_{nom,i}) - C_w(Q_{nom,i-1})}{E_{pv} c_e} \qquad (15)$$

Fig. 11(a) reports γ as a function of Θ showing a similar trend compared to λ (Fig. 10(b)). Also in this case, $\gamma \simeq -20\%$ for $\Theta = 1.2\,\mathrm{h}$ then the curves flatten almost immediately around zero after a short plateau around -5%. In 2010, Li-Ion battery pack prices were above $1100\,\$/\mathrm{kWh}$ and have fallen to $137\,\$/\mathrm{kWh}$ in 2020 (89% reduction in real terms) [90]. This is equivalent to $c_b = 112.65\,€/\mathrm{kWh}$, according to the 2020 reference exchange rates [91]. By 2023, the average prices will be close to $100\,\$/\mathrm{kWh}$, according to the latest forecast by BloombergNEF (BNEF) [90]. In this economic analysis that focuses on the interaction between residential building, battery, and grid, we assume that the energy fed into the grid is not paid for. In fact, its economic value is dominated by country-specific subsidiary mechanisms that would hinder a general analysis. Moreover, battery energy storage system should have the objective to maximize the self-consumption of locally produced renewable energy. Such an objective would be put in background by very generous subsidiary mechanism for the electricity eventually sold to the grid.

To evaluate the feasibility of the BESS investment, we analyze the Pay Back Period PBP :

$$\mathrm{PBP} = \frac{I_i}{S_a}\,, \qquad (16)$$

where $I_i = Q_{nom}\, c_b$ is the initial investment for the battery and S_a is the annual saving due to the reduction of the energy withdrawn from the grid generated by the BESS. Fig. 11(b) shows PBP as a function of Θ for all the climates. The moderate climate has the lowest PBP while the cold climate has the highest one. The other three climates have approximately the same PBP. We observe that PBP grows almost linearly for $\Theta > 2\,\mathrm{h}$ because the initial investment for the battery dominates compared to S_a. For $\Theta \simeq 3.5\,\mathrm{h}$, PBP is between 2.5 years (moderate climate) and 4.7 years (cold climate). Therefore, using λ curves to optimally size the battery returns a sustainable investment for all climates. Conversely, using the BESS for seasonal storage is unsustainable either with current batteries costs nor with those reasonably foreseeable in the short-medium term.

4.2. Discussion

Besides determining the optimal techno-economic size of the battery, our methodology allows to dissect its operation as a function of the climatic conditions.

We first consider the average BESS State of Charge (SoC_m) as an indicator of the system utilization factor. Comparing Table 7 to Fig. 11(b) we observe that SoC_m correlates with the climatic variation of PBP. Specifically, the pay back period is inversely proportional to SoC_m. Cold and Moderate climates have the lowest and highest SoC_m, respectively. This is coherent with their PBP trends (Fig. 11). Conversely, heating based, cooling based, and hot climates have similar SoC_m and their pay back period curves collapse on the same pattern (Fig. 11).

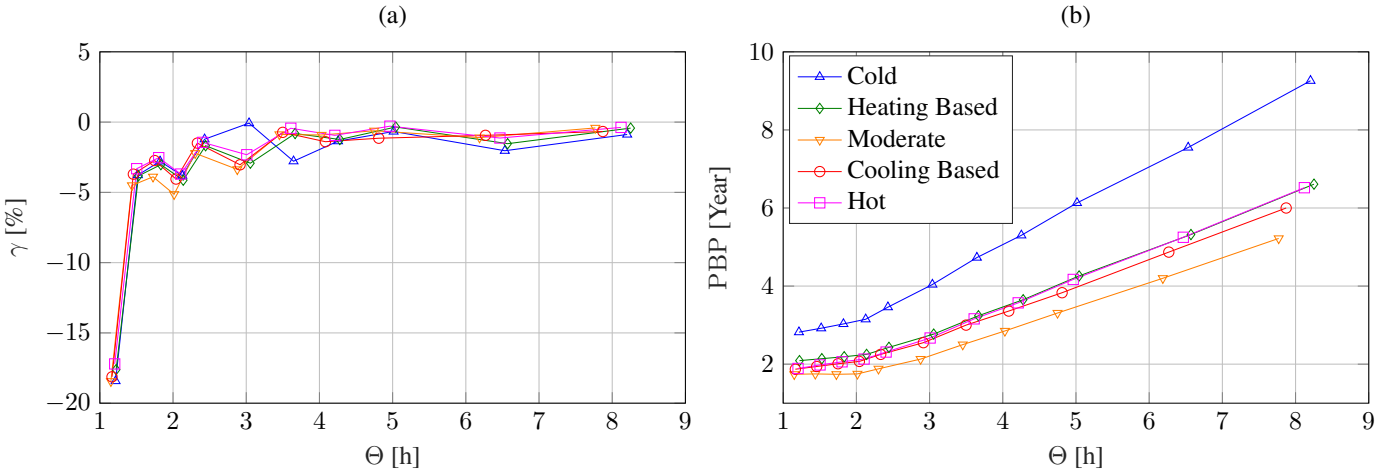

Figure 11: (a) γ as a function Θ; (b) PayBack Period as a function of Θ.

Such an analysis supports the conclusion that, for nZEB applications, BESSs are not suitable for seasonal storage. In fact, long term storage requires large capacities but the SoC_m decreases as Q_{nom} increases, consequently yielding a larger pay back period. Similar results are obtained in [64] that shows that the investment cost steadily rises with battery size, and that PBP is shorter for smaller capacity systems. In addition to this, our results provide a general criterion for the techno-economic optimization of the BESS capacity.

Climatic Zone	SoC_m	E_s/U_{tot}
Cold	0.29	0.41
Heating based	0.37	0.76
Moderate	0.53	1.00
Cooling based	0.39	0.73
Hot	0.40	0.68

Table 7: Average annual State of Charge and renewable electricity self consumption for $\Theta = 3.5\,\mathrm{h}$.

The pay back period also correlates to the share of the building demand fulfilled by local RES, $\Xi = E_s/U_{tot}$, (Tab. 7) as highlighted in [66]. Therein, it is shown that BESSs are highly profitable when the combination between the supply and the demand allows a significant increase of energy self-consumption. Similarly, we found that larger Ξ positively impact the PBP (Tab. 7). The imbalance between PV production and building demand :

$$D = |P_{pv}(t) - u_{tot}(t)|\,, \tag{17}$$

largely determines the battery operation, the λ and γ values, and, finally, the battery optimal capacity. D exhibits the same frequency histogram for all the climates (Fig. 12). As a consequence, the temporal mismatch between the P_{pv} and u_{tot} is similar for all the climates, despite they have different F values (Tab. 5). All diagrams exhibit a major frequency peak for $D \simeq 3\,\mathrm{kW}$ generally followed by a lower peak for $10\,\mathrm{kW} < D < 15\,\mathrm{kW}$. This, explains the patterns reported in Fig. 10 and 11 suggesting also that F has a minor impact on the BESS operation. In fact, the optimal sizing of the battery is related to the temporal mismatch between P_{pv} and u_{tot}, and by the D frequency diagram. On the contrary, F compares the total energy produced by the renewable energy sources to the nZEB yearly demand, but does not provide information nor on their instantaneous difference nor on their discrepancy in time.

To this end, Fig. 13 shows the SoC as a function of time for all the climates and for $\Theta = 3.5\,\mathrm{h}$. Generally, the battery is most likely to reach a high state of charge in transitional seasons when u_{tot} is commonly lower than P_{pv} (Fig. 9). Specifically, in cold climate, the BESS is discharged for all winter and part of fall and spring, when the SoC is steadily about 10% and without significant cycling (Fig. 13(a)). In the rest of the year, the SoC exhibits a clear daily cycling with relatively large values during the central part of the day. In fact, in this climate, u_h prevails over the other demands causing a large energy demand in the colder periods (Tab. 5). As a result, the battery is unused for about 100 days per year, concentrated in colder seasons. This further explains why the cold climate has the largest PBP: the low SoC_m results from a relatively long period of BESS disuse (about $1/3$ of the year), rather then from and average low SoC. As a consequence the pay back period is $1/3$ longer than the average of other climates (Fig. 11(b)).

In heating based climate (Fig. 13(b)), the BESS has a steadily low SoC only for less than 30 days during summer. For the rest of the year there is a clear daily SoC cycling, indicating that the battery is effectively used to match photovoltaic production and nZEB demand. The highest SoC occurs during fall and spring, when it generally varies between 50% and 90%. In winter the state of charge is lower, in particular during late night and before noon. However, during such a cold season, the SoC varies between 10% and 90% showing a deeper cycling compared to warmer seasons. Only during transitional periods, SoC is consistently high at the evening, and energy is transferred to the following morning. The summer disuse period, causes such a climate to have the second longest PBP (Fig. 11(b)).

In moderate climate the BESS has almost the same behavior throughout the whole year (Fig. 13(c)). It is charged during the

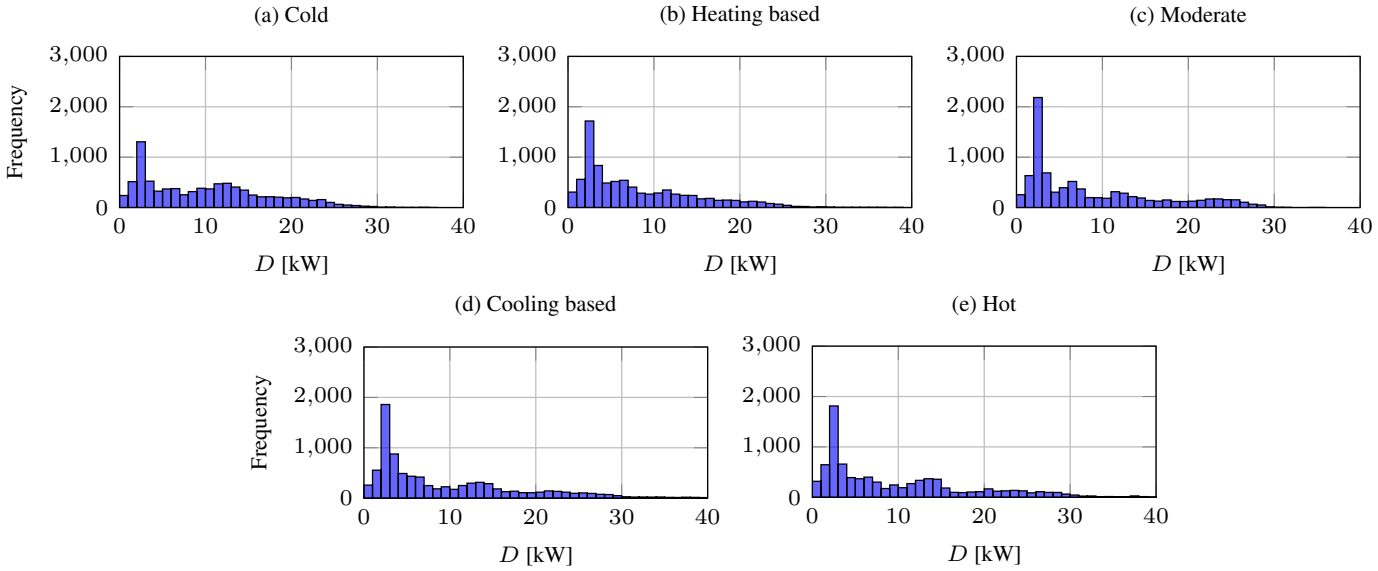

Figure 12: D Frequency histograms: (a) Cold climate; (b) heating based climate; (c) moderate climate; (d) cooling based climate; and (e) hot climate.

central hours of the day, reaching high state of charge and then discharged in the evening and during the morning. The SoC cycles between 35% and 90% during hot and transitional seasons, and between 10% and 90% during cold periods. At night, generally, SoC $> 40\%$ and residual energy is used during the subsequent morning. As a consequence the minimum state of charge locates at late morning (just before noon). This is particularly evident for the colder periods, when the PV production is lower in particular at morning.

In cooling based climate, the BESS is always used. In fact, even during summer, when SoC $< 40\%$ for about 60 days, Fig. 13(c) evidences daily a SoC cycling. State of charge is always maximum after noon. During transitional seasons, residual SoC in the evening (SoC $> 50\%$), is used to satisfy the demand in the morning. Conversely, during summer, at night the battery is already completely discharged due to the large cooling energy demand (Fig. 9). Cold periods, exhibit a more variable behavior where SoC at the evening varies between 10% and 40%. Overall, such a battery usage pattern returns the second shorter pay back period (Fig.11(b)).

Hot climate exhibits a SoC pattern similar to cooling based climate. Yet, the hot season is much longer and the state of charge remains below 40% for about 100 days. This reduces the effectiveness of the battery and yields a longer PBP, similar to that of the heating based climate.

SoC patterns show that the BESS never consistently charges during one season and discharges during another. Rather, it is always characterized by a daily state of charge cycling. This is consistent with and supports the results of Fig. 10(b) and 11(b). Therein, $\Theta = 3.5$ h was identified as the optimal techno-economic size for the battery that qualifies as a daily storage solution for nZEB (see also [63, 64] for similar conclusions). In fact, the BESS allows matching the PV production and nZEB demand within a day (Fig. 13). Notably, such optimized battery storage increases the percentage of the nZEB energy consumption supplied by RES by roughly 50%. Similar results are also reported in [67] for different RES scenarios in typical high-rise building in Hong Kong. Moreover, our results allow analyzing the BESS impact the RES consumption share for diverse climates. Specifically, the hot climate shows the largest increment (56%), the cold, heating based and cooling based climates are all close to 50%, whereas the moderate climate exhibits the lowest one (35%). In the moderate climate, the low increment is explained considering that for $\Theta = 3.5$ h PV already completely fulfill the energy demand.

Results show that building level electricity storage cannot completely match production and demand, even when $F < 1$. Other technologies (i.e. grid or sub-grid level storage) are required to further increase the self consumption share of the locally produces renewable energy. Electric mobility is one of such technologies. The Nissan Leaf consumes $20.6\,\text{kWh}/100\,\text{km}$ [92]. In Europe, the average daily distance traveled by a car is about 33 km [93], that results in an average energy required to recharge a car of about 2481 kWh per year. Therefore, the PV energy that cannot be locally used, could be exploited to fully recharge from a minimum of 2 vehicles (cold climate) to a maximum of almost 7 vehicles (moderate climate). The emission limits for a EURO 6 diesel vehicle are $g_{CO_2} = 95$ g/km [94], $g_{CO} = 0.5$ g/km [95], $g_{NO_x} = 0.08$ g/km [95], $g_{PM} = 0.005$ g/km [95]. Thus, this solution would avoid the release into the atmosphere of a minimum of about $G_{CO_2} = 1945$ kg/year , $G_{CO} = 10$ kg/year, $G_{NO_x} = 1.6$ kg/year, $G_{PM} = 0.1$ kg/year (cold climate) to a maximum of about $G_{CO_2} = 7815$ kg/year, $G_{CO} = 41$ kg/year, $G_{NO_x} = 6.6$ kg/year, $G_{PM} = 0.4$ kg/year (moderate climate). Vehicle energy storage, can be effectively integrated into the nZEB as demonstrated in [96].

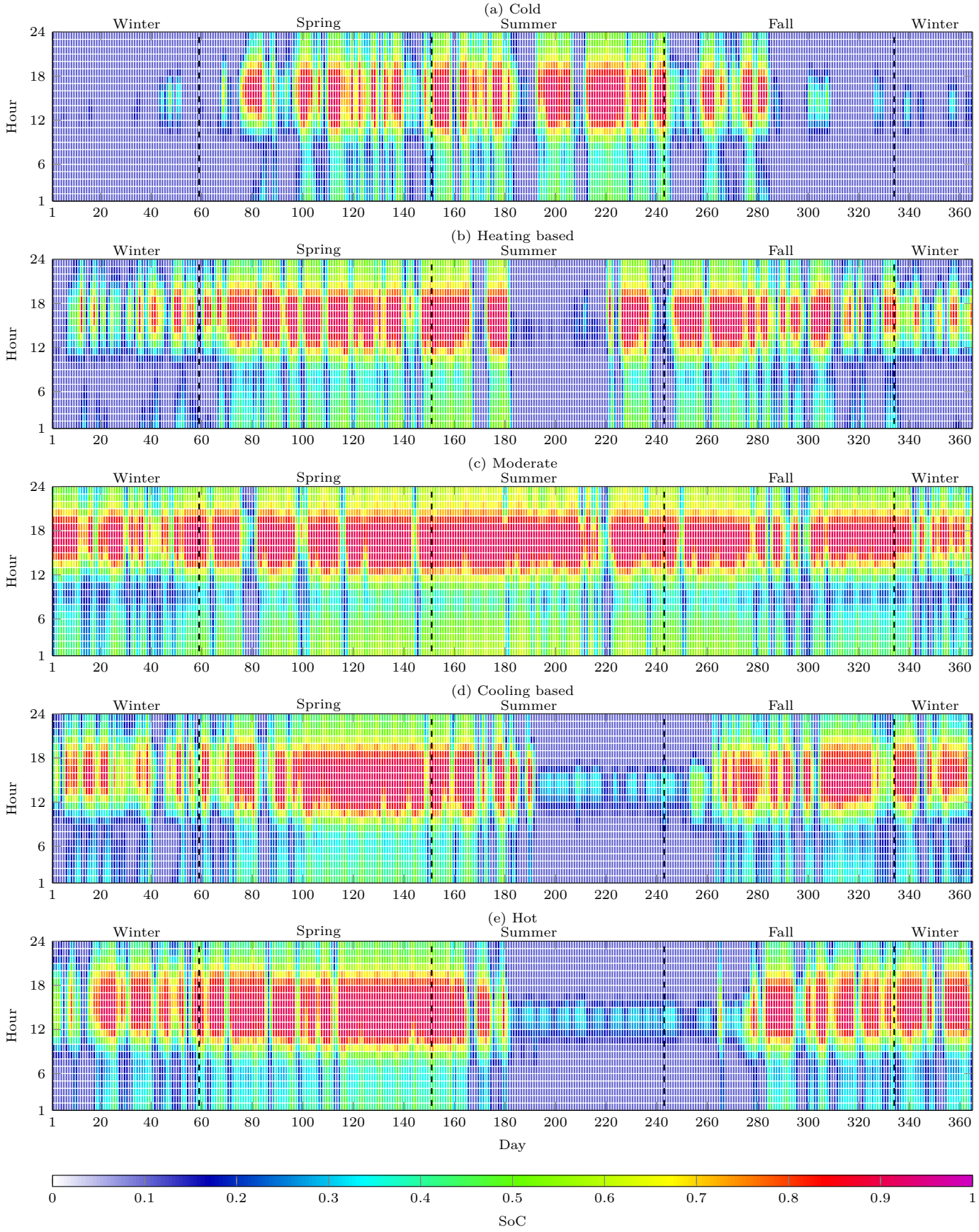

Figure 13: State of Charge of the Li-Ion battery as a function of time for (a) Cold climate; (b) Heating based climate; (c) Moderate climate; (d) Cooling based climate; (e) Hot climate.

5. Conclusions

In this paper we assess a climate independent scaling law for the optimization of a BESS in a residential environment. We evaluate the environmental and economic impact of the integration of a Li-Ion battery based electricity storage in a real existing nZEB, for five different climates and for different battery capacities. We optimize the system control in order to maximize the share of self consumed renewable energy for all configurations. We model the demand of the residential building for each climate through the "EnergyPlus" software. We determine the PV production with the "PVGIS" platform. In addition, we model the Li-Ion battery trough the zero-th order equivalent circuit presented in [79]. Consumption data are validated against measured energy demands.

We leverage on such data and models to carry out a techno-economic analysis of battery integration for five different climates and for twelve different battery capacities. We evaluate the self-consumed energy, his relative variation and the relative variation of the cost of energy withdrawn from the grid, as a function of the relative battery capacity. These representations correlate all the most significant energy quantities of the plant.

The results highlight that a relative battery capacity $1.5\,\mathrm{h} < \Theta < 3.5\,\mathrm{h}$ is the best solution from an energy and economical point of view. We observe that the selected design criterion yields a PBP between 1.8 years (moderate climate) and 4.7 years (cold climate). In conclusion, such an investment is sustainable and gathers significant advantages both on an energy and environmental level, for all the climates analyzed.

The methodology is also used to dissect the hourly operation of the optimized battery. This analysis, demonstrates that, in the nZEB scenario, the BESS qualifies as a daily storage system. In fact, allows matching the photovoltaic production and building consumption on a daily basis. Conversely, the battery never consistently charges during one season and discharges during another not even when $\Xi < 1$ and $E_s < E_{pv}$. This highlights the possibility/necessity to combine BESSs with different technologies, possibly grid or sub-grid level storage. Electric vehicles could effectively be one of such technologies.

In our vision, the presented framework is a valuable tool for the preliminary design of batteries in buildings. On the one hand, the design of such systems should leverage on instantaneous energy consumption and production data. On the other hand the scaling laws presented in Fig. 10 and 11 greatly simplify BESSs sizing requiring only the maximum renewable energy sources production as input. Designing BESSs according to the results herein presented yields both a sustainable investment and an effective solution in terms of RES exploitation and limitation of grid issues. Moreover, the battery and nZEB models, are valuable tools for policy makers to determine pricing policies that optimize specific objective functions such as to maximize the renewable energy sources exploitation. A further feasible application is utilizing the proposed battery model for the design of the battery. In fact, such model allows selecting the number of the cells, their connection (number of cells in parallel and in series), the battery volume, and cooling surface. To this end, the model could be ameliorated by implementing a more detailed thermal management. So far, battery self-discharge has been discarded. Its impact on the present results are negligible due to the low storage duration. However, such a phenomenon should be considered for longer (i.e. seasonal) storage. Finally, our results leverage on a rule based strategy for system control. Using an optimized strategy could further improve the framework effectiveness.

Acknowledgment

The present research work has been supported by the Italian Ministry of Education, Universities and Research, MIUR, as Project of National Interest, PRIN 2017F4S2L3 and by the project "Efficienza energetica negli edifici: un approccio integrato verso l'edificio a zero emissioni" founded by Regione Lazio, POR-FESR 2014-2020, call "interventi per il rafforzamento della ricerca nel Lazio - incentivi per i dottorati di innovazione per le imprese Asse 3 - Istruzione e formazione - Priorità di investimento 10 ii) Obiettivo specifico 10.5 Azione Cardine 21.

The Authors would also like to Acknowledge Saggini Costruzioni for the fruitful collaboration and for the data provided to this research.

References

[1] A. Gallo, J. Simões-Moreira, H. Costa, M. Santos, E. M. dos Santos, Energy storage in the energy transition context: A technology review, Renewable and sustainable energy reviews 65 (2016) 800–822.

[2] V. Olkkonen, J. Ekström, A. Hast, S. Syri, Utilising demand response in the future finnish energy system with increased shares of baseload nuclear power and variable renewable energy, Energy 164 (2018) 204–217.

[3] R. L. Arantegui, A. Jäger-Waldau, Photovoltaics and wind status in the european union after the paris agreement, Renewable and Sustainable Energy Reviews 81 (2018) 2460–2471.

[4] P. Mancarella, Mes (multi-energy systems): An overview of concepts and evaluation models, Energy 65 (2014) 1–17.

[5] P. Gabrielli, M. Gazzani, E. Martelli, M. Mazzotti, Optimal design of multi-energy systems with seasonal storage, Applied Energy 219 (2018) 408–424.

[6] M. Wirtz, M. Hahn, T. Schreiber, D. Müller, Design optimization of multi-energy systems using mixed-integer linear programming: Which model complexity and level of detail is sufficient?, Energy Conversion and Management 240 (2021) 114249.

[7] G. Hug-Glanzmann, Coordination of intermittent generation with storage, demand control and conventional energy sources, in: 2010 IREP Symposium Bulk Power System Dynamics and Control-VIII (IREP), IEEE, 2010, pp. 1–7.

[8] J. M. Carrasco, L. G. Franquelo, J. T. Bialasiewicz, E. Galván, R. C. PortilloGuisado, M. M. Prats, J. I. León, N. Moreno-Alfonso, Power-electronic systems for the grid integration of renewable energy sources: A survey, IEEE Transactions on industrial electronics 53 (4) (2006) 1002–1016.

[9] M. Liserre, T. Sauter, J. Y. Hung, Future energy systems: Integrating renewable energy sources into the smart power grid through industrial electronics, IEEE industrial electronics magazine 4 (1) (2010) 18–37.

[10] M. A. Eltawil, Z. Zhao, Grid connected photovoltaic power systems: Technical and potential problems a review, Renewable and sustainable energy reviews 14 (1) (2010) 112–129.

[11] J. Koskela, A. Rautiainen, P. Järventausta, Using electrical energy storage in residential buildings–sizing of battery and photovoltaic panels based on electricity cost optimization, Applied energy 239 (2019) 1175–1189.

[12] P. D. Lund, J. Lindgren, J. Mikkola, J. Salpakari, Review of energy system flexibility measures to enable high levels of variable renewable electricity, Renewable and sustainable energy reviews 45 (2015) 785–807.

[13] M. T. Turan, Y. Ates, O. Erdinc, E. Gokalp, J. P. Catalão, Effect of electric vehicle parking lots equipped with roof mounted photovoltaic panels on the distribution network, International Journal of Electrical Power & Energy Systems 109 (2019) 283–289.

[14] H. Farhangi, The path of the smart grid, IEEE power and energy magazine 8 (1) (2009) 18–28.

[15] E. F. Camacho, T. Samad, M. Garcia-Sanz, I. Hiskens, Control for renewable energy and smart grids, The Impact of Control Technology, Control Systems Society 4 (8) (2011) 69–88.

[16] T. M. Lawrence, M.-C. Boudreau, L. Helsen, G. Henze, J. Mohammadpour, D. Noonan, D. Patteeuw, S. Pless, R. T. Watson, Ten questions concerning integrating smart buildings into the smart grid, Building and Environment 108 (2016) 273–283.

[17] H. Hashemi-Dezaki, S. M. M. Agah, H. Askarian-Abyaneh, H. Haeri-Khiavi, Sensitivity analysis of smart grids reliability due to indirect cyber-power interdependencies under various dg technologies, dg penetrations, and operation times, Energy Conversion and Management 108 (2016) 377–391.

[18] Y. Ateş, T. Gökçek, A. Y. Arabul, Impact of hybrid power generation on voltage, losses, and electricity cost in distribution networks, Turkish Journal of Electrical Engineering & Computer Sciences 29 (3) (2021) 1720–1735.

[19] D. Mohler, D. Sowder, Energy storage and the need for flexibility on the grid, in: Renewable energy integration, Elsevier, 2017, pp. 309–316.

[20] E. Shove, Time to rethink energy research, Nature Energy 6 (2) (2021) 118–120.

[21] Y. Zhang, X. Bai, F. P. Mills, J. C. Pezzey, Rethinking the role of occupant behavior in building energy performance: A review, Energy and Buildings 172 (2018) 279–294.

[22] G. Stuart, P. Fleming, V. Ferreira, P. Harris, Rapid analysis of time series data to identify changes in electricity consumption patterns in uk secondary schools, Building and Environment 42 (4) (2007) 1568–1580.

[23] A. L. Facci, L. Andreassi, S. Ubertini, Optimization of chcp (combined heat power and cooling) systems operation strategy using dynamic programming, Energy 66 (2014) 387–400.

[24] A. L. Facci, L. Andreassi, S. Ubertini, E. Sciubba, Analysis of the influence of thermal energy storage on the optimal management of a trigeneration plant, Energy procedia 45 (2014) 1295–1304.

[25] A. L. Facci, V. K. Krastev, G. Falcucci, S. Ubertini, Smart integration of photovoltaic production, heat pump and thermal energy storage in residential applications, Solar Energy 192 (2019) 133–143.

[26] A. L. Facci, S. Ubertini, Analysis of a fuel cell combined heat and power plant under realistic smart management scenarios, Applied Energy 216 (2018) 60–72.

[27] A. L. Facci, S. Ubertini, Meta-heuristic optimization for a high-detail smart management of complex energy systems, Energy Conversion and Management 160 (2018) 341–353.

[28] E. O'Shaughnessy, D. Cutler, K. Ardani, R. Margolis, Solar plus: Optimization of distributed solar pv through battery storage and dispatchable load in residential buildings, Applied Energy 213 (2018) 11–21.

[29] N. Kittner, F. Lill, D. M. Kammen, Energy storage deployment and innovation for the clean energy transition, Nature Energy 2 (9) (2017) 1–6.

[30] L. Tziovani, P. Kolios, L. Hadjidemetriou, E. Kyriakides, Energy scheduling in non-residential buildings integrating battery storage and renewable solutions, in: 2018 IEEE International Energy Conference (ENERGYCON), IEEE, 2018, pp. 1–6.

[31] D. Howell, B. Cunningham, T. Duong, P. Faguy, Overview of the doe vto advanced battery r&d program, Department of Energy (2016).

[32] H. Chen, T. N. Cong, W. Yang, C. Tan, Y. Li, Y. Ding, Progress in electrical energy storage system: A critical review, Progress in natural science 19 (3) (2009) 291–312.

[33] C. Zhang, Y.-L. Wei, P.-F. Cao, M.-C. Lin, Energy storage system: Current studies on batteries and power condition system, Renewable and Sustainable Energy Reviews 82 (2018) 3091–3106.

[34] P. E. Campana, L. Cioccolanti, B. François, J. Jurasz, Y. Zhang, M. Varini, B. Stridh, J. Yan, Li-ion batteries for peak shaving, price arbitrage, and photovoltaic self-consumption in commercial buildings: A monte carlo analysis, Energy Conversion and Management 234 (2021) 113889.

[35] Y. Yang, S. Bremner, C. Menictas, M. Kay, Battery energy storage system size determination in renewable energy systems: A review, Renewable and Sustainable Energy Reviews 91 (2018) 109–125.

[36] W. Nam, J.-Y. Kim, K.-Y. Oh, The characterization of dynamic behavior of li-ion battery packs for enhanced design and states identification, Energy Conversion and Management 162 (2018) 264–275.

[37] I. Worighi, T. Geury, M. El Baghdadi, J. Van Mierlo, O. Hegazy, A. Maach, Optimal design of hybrid pv-battery system in residential buildings: End-user economics, and pv penetration, Applied Sciences 9 (5) (2019) 1022.

[38] J. Li, Optimal sizing of grid-connected photovoltaic battery systems for residential houses in australia, Renewable energy 136 (2019) 1245–1254.

[39] F. R. S. Sevilla, D. Parra, N. Wyrsch, M. K. Patel, F. Kienzle, P. Korba, Techno-economic analysis of battery storage and curtailment in a distribution grid with high pv penetration, Journal of Energy Storage 17 (2018) 73–83.

[40] M. Bortolini, M. Gamberi, A. Graziani, Technical and economic design of photovoltaic and battery energy storage system, Energy Conversion and Management 86 (2014) 81–92.

[41] M. Guezgouz, J. Jurasz, B. Bekkouche, T. Ma, M. S. Javed, A. Kies, Optimal hybrid pumped hydro-battery storage scheme for off-grid renewable energy systems, Energy Conversion and Management 199 (2019) 112046.

[42] A. Joseph, M. Shahidehpour, Battery storage systems in electric power systems, in: 2006 IEEE Power Engineering Society General Meeting, IEEE, 2006, pp. 8–pp.

[43] N. Garimella, N.-K. C. Nair, Assessment of battery energy storage systems for small-scale renewable energy integration, in: TENCON 2009-2009 IEEE region 10 conference, IEEE, 2009, pp. 1–6.

[44] R. Velik, The influence of battery storage size on photovoltaics energy

self-consumption for grid-connected residential buildings, IJARER International Journal of Advanced Renewable Energy Research 2 (6) (2013).
[45] B. Nykvist, M. Nilsson, Rapidly falling costs of battery packs for electric vehicles, Nature climate change 5 (4) (2015) 329–332.
[46] D. D'agostino, P. Zangheri, L. Castellazzi, Towards nearly zero energy buildings in europe: A focus on retrofit in non-residential buildings, Energies 10 (1) (2017) 117.
[47] ECA, Energy efficiency in buildings: greater focus on cost-effectiveness still needed., https://op.europa.eu/webpub/eca/special-reports/energy-efficiency-11-2020/en/ Accessed on 20.12.2021.
[48] G. Merei, J. Moshövel, D. Magnor, D. U. Sauer, Optimization of self-consumption and techno-economic analysis of pv-battery systems in commercial applications, Applied Energy 168 (2016) 171–178.
[49] S. Antvorskov, Introduction to integration of renewable energy in demand controlled hybrid ventilation systems for residential buildings, Building and Environment 43 (8) (2008) 1350–1353.
[50] P. M. Congedo, C. Baglivo, D. D'Agostino, I. Zacà, Cost-optimal design for nearly zero energy office buildings located in warm climates, Energy 91 (2015) 967–982.
[51] M. Kapsalaki, V. Leal, M. Santamouris, A methodology for economic efficient design of net zero energy buildings, Energy and Buildings 55 (2012) 765–778.
[52] Y. Lu, S. Wang, K. Shan, Design optimization and optimal control of grid-connected and standalone nearly/net zero energy buildings, Applied Energy 155 (2015) 463–477.
[53] P. Chastas, T. Theodosiou, K. J. Kontoleon, D. Bikas, Normalising and assessing carbon emissions in the building sector: A review on the embodied co2 emissions of residential buildings, Building and Environment 130 (2018) 212–226.
[54] P. Chastas, T. Theodosiou, D. Bikas, Embodied energy in residential buildings-towards the nearly zero energy building: A literature review, Building and environment 105 (2016) 267–282.
[55] M. Conci, T. Konstantinou, A. van den Dobbelsteen, J. Schneider, Trade-off between the economic and environmental impact of different decarbonisation strategies for residential buildings, Building and Environment 155 (2019) 137–144.
[56] A. Martinez, S. D. de Garayo, P. Aranguren, D. Astrain, Assessing the reliability of current simulation of thermoelectric heat pumps for nearly zero energy buildings: Expected deviations and general guidelines, Energy Conversion and Management 198 (2019) 111834.
[57] S. Attia, P. Eleftheriou, F. Xeni, R. Morlot, C. Ménézo, V. Kostopoulos, M. Betsi, I. Kalaitzoglou, L. Pagliano, M. Cellura, et al., Overview and future challenges of nearly zero energy buildings (nzeb) design in southern europe, Energy and Buildings 155 (2017) 439–458.
[58] F. Asdrubali, I. Ballarini, V. Corrado, L. Evangelisti, G. Grazieschi, C. Guattari, Energy and environmental payback times for an nzeb retrofit, Building and Environment 147 (2019) 461–472.
[59] M. M. Sesana, G. Salvalai, Overview on life cycle methodologies and economic feasibility for nzebs, Building and Environment 67 (2013) 211–216.
[60] G. Tumminia, F. Guarino, S. Longo, D. Aloisio, S. Cellura, F. Sergi, G. Brunaccini, V. Antonucci, M. Ferraro, Grid interaction and environmental impact of a net zero energy building, Energy Conversion and Management 203 (2020) 112228.
[61] S. Cao, K. Sirén, Matching indices taking the dynamic hybrid electrical and thermal grids information into account for the decision-making of nzeb on-site renewable energy systems, Energy Conversion and Management 101 (2015) 423–441.
[62] D. D'Agostino, L. Mazzarella, What is a nearly zero energy building? overview, implementation and comparison of definitions, Journal of Building Engineering 21 (2019) 200–212.
[63] Y. Zhang, A. Lundblad, P. E. Campana, J. Yan, Employing battery storage to increase photovoltaic self-sufficiency in a residential building of sweden, Energy Procedia 88 (2016) 455–461.
[64] M. Akter, M. Mahmud, A. M. Oo, Comprehensive economic evaluations of a residential building with solar photovoltaic and battery energy storage systems: An australian case study, Energy and Buildings 138 (2017) 332–346.
[65] E. Tervo, K. Agbim, F. DeAngelis, J. Hernandez, H. K. Kim, A. Odukomaiya, An economic analysis of residential photovoltaic systems with lithium ion battery storage in the united states, Renewable and Sustainable Energy Reviews 94 (2018) 1057–1066.
[66] F. Cucchiella, I. D'adamo, M. Gastaldi, Photovoltaic energy systems with battery storage for residential areas: an economic analysis, Journal of Cleaner Production 131 (2016) 460–474.
[67] J. Liu, M. Wang, J. Peng, X. Chen, S. Cao, H. Yang, Techno-economic design optimization of hybrid renewable energy applications for high-rise residential buildings, Energy Conversion and Management 213 (2020) 112868.
[68] J. Liu, X. Chen, H. Yang, Y. Li, Energy storage and management system design optimization for a photovoltaic integrated low-energy building, Energy 190 (2020) 116424.
[69] X. Liu, N. Iftikhar, H. Huo, R. Li, P. S. Nielsen, Two approaches for synthesizing scalable residential energy consumption data, Future Generation Computer Systems 95 (2019) 586–600.
[70] T. Ahmad, H. Chen, Y. Guo, J. Wang, A comprehensive overview on the data driven and large scale based approaches for forecasting of building energy demand: A review, Energy and Buildings 165 (2018) 301–320.
[71] U. Desideri, L. Arcioni, D. Leonardi, L. Cesaretti, P. Perugini, E. Agabitini, N. Evangelisti, Design of a multipurpose "zero energy consumption" building according to european directive 2010/31/eu: Architectural and technical plants solutions, Energy 58 (2013) 157–167.
[72] Y. Schmitt, A. Troi, G. P. W. Sparber, Klimahaus casaclima–a regional energy certification system stimulates low energy architecture, in: Proceedings of PLEA2007-The 24th Conference on Passive and Low Energy Architecture, Singapore, 2007, pp. 22–24.
[73] A. Magrini, G. Lentini, S. Cuman, A. Bodrato, L. Marenco, From nearly zero energy buildings (nzeb) to positive energy buildings (peb): The next challenge-the most recent european trends with some notes on the energy analysis of a forerunner peb example, Developments in the Built Environment 3 (2020) 100019.
[74] N. Omar, M. Daowd, O. Hegazy, G. Mulder, J.-M. Timmermans, T. Coosemans, P. Van den Bossche, J. Van Mierlo, Standardization work for bev and hev applications: Critical appraisal of recent traction battery documents, Energies 5 (1) (2012) 138–156.
[75] J. Laustsen, Energy efficiency requirements in building codes, energy efficiency policies for new buildings. iea information paper (2008).
[76] Energyplus, https://energyplus.net/ Accessed on 20.12.2021.
[77] R. McKenna, E. Merkel, W. Fichtner, Energy autonomy in residential buildings: A techno-economic model-based analysis of the scale effects, Applied Energy 189 (2017) 800–815.
[78] E. Commission, Photovoltaic geographical information system., https://re.jrc.ec.europa.eu/pvg_tools/it/#PVP Accessed on 20.12.2021.
[79] S. Onori, L. Tribioli, Adaptive pontryagin s minimum principle supervisory controller design for the plug-in hybrid gm chevrolet volt, Applied Energy 147 (2015) 224–234.
[80] N. Kim, S. Cha, H. Peng, Optimal control of hybrid electric vehicles based on pontryagin's minimum principle, IEEE Transactions on control systems technology 19 (5) (2010) 1279–1287.
[81] G. L. Plett, Sigma-point kalman filtering for battery management systems of lipb-based hev battery packs: Part 2: Simultaneous state and parameter estimation, Journal of power sources 161 (2) (2006) 1369–1384.
[82] R. Willis, Principles of mechanism, Longmans, Green, Harlow, 1870.
[83] S. K. Mohammadian, Y. Zhang, Thermal management optimization of an air-cooled li-ion battery module using pin-fin heat sinks for hybrid electric vehicles, Journal of Power Sources 273 (2015) 431–439.
[84] Marklines, Nissan leaf teardown: Lithium-ion battery pack structure, https://www.marklines.com/en/report_all/rep1786_201811 Accessed on 20.12.2021.
[85] L. Guzzella, A. Sciarretta, et al., Vehicle propulsion systems, Vol. 1, Springer, New York City, 2007.
[86] D. Parra, M. K. Patel, Effect of tariffs on the performance and economic benefits of pv-coupled battery systems, Applied energy 164 (2016) 175–187.
[87] V. Ciancio, S. Falasca, I. Golasi, G. Curci, M. Coppi, F. Salata, Influence of input climatic data on simulations of annual energy needs of a building: Energyplus and wrf modeling for a case study in rome (italy), Energies 11 (10) (2018) 2835.
[88] J. H. Yoon, R. Baldick, A. Novoselac, Dynamic demand response controller based on real-time retail price for residential buildings, IEEE

Transactions on Smart Grid 5 (1) (2014) 121–129.
[89] Eurostat, Electricity price statistics, https://ec.europa.eu/eurostat/statistics-explained/index.php?title=Electricity_price_statistics Accessed on 20.12.2021.
[90] BNEF, Battery pack prices cited below 100 $/kwh for the first time in 2020, while market average sits at 137 $/kwh.
[91] B. D'Italia, Cambi di riferimento del 14 dicembre 2020, https://www.bancaditalia.it/compiti/operazioni-cambi/cambio/cambi_rif_20201214/ Accessed on 20.12.2021.
[92] Wltp - nissan leaf, https://www-europe.nissan-cdn.net/content/dam/Nissan/ch/it/brochures/pkw/leaf-2018-brochure-listino-prezzi.pdf Accessed on 20.12.2021.
[93] Change in distance travelled by car, https://www.odyssee-mure.eu/publications/efficiency-by-sector/transport/distance-travelled-by-car.html Accessed on 20.12.2021.
[94] Co2 emission performance standards for cars and vans, https://ec.europa.eu/clima/policies/transport/vehicles/regulation_en Accessed on 20.12.2021.
[95] E. Parliament, Regulation (ec) no 715/2007 of the european parliament and of the council of 20 june 2007 on type approval of motor vehicles with respect to emissions from light passenger and commercial vehicles (euro 5 and euro 6) and on access to vehicle repair and maintenance information (text with eea relevance).
[96] A. Rosati, G. Loreti, A. L. Facci, J. Taborri, S. Rossi, S. Ubertini, Smart energy community for electric vehicles recharge in a building environment, in: 13th International Conference on Applied Energy ICAE-2021, ICAE, 2021.